

Paleogene equatorial penguins challenge the proposed relationship between biogeography, diversity, and Cenozoic climate change

Julia A. Clarke^{a,b,c,d}, Daniel T. Ksepka^c, Marcelo Stucchi^e, Mario Urbina^f, Norberto Giannini^{g,h}, Sara Bertelli^{i,g}, Yanina Narváez^j, and Clint A. Boyd^a

^aDepartment of Marine, Earth, and Atmospheric Sciences, North Carolina State University, Campus Box 8208, Raleigh, NC 27695; ^bDepartment of Paleontology, North Carolina Museum of Natural Sciences, 11 West Jones Street, Raleigh, NC 27601-1029; Divisions of ^cPaleontology and ^dVertebrate Zoology, American Museum of Natural History, Central Park West at 79th Street, New York, NY 10024; ^eAsociación para la Investigación y Conservación de la Biodiversidad, Los Agrólogos 220, Lima 12, Perú; ^fDepartment of Vertebrate Paleontology, Museo de Historia Natural, Universidad Nacional Mayor de San Marcos, Avenida Arenales 1256, Lima 14, Perú; ^gPrograma de Investigaciones de Biodiversidad Argentina (Consejo Nacional de Investigaciones Científicas y Técnicas), Facultad de Ciencias Naturales, Instituto Miguel Lillo de la Universidad Nacional de Tucumán, Miguel Lillo 205, CP 4000, Tucumán, Argentina; ^hThe Dinosaur Institute, Natural History Museum of Los Angeles County, 900 Exposition Boulevard, Los Angeles, CA 90007; and ⁱDepartment of Geology, Centro de Investigación Científica y de Educación Superior de Ensenada, Kilometer 107 Carretera Tijuana–Ensenada, 22860 Ensenada, Baja California, México

Edited by R. Ewan Fordyce, University of Otago, Dunedin, New Zealand, and accepted by the Editorial Board May 21, 2007 (received for review December 14, 2006)

New penguin fossils from the Eocene of Peru force a reevaluation of previous hypotheses regarding the causal role of climate change in penguin evolution. Repeatedly it has been proposed that penguins originated in high southern latitudes and arrived at equatorial regions relatively recently (e.g., 4–8 million years ago), well after the onset of latest Eocene/Oligocene global cooling and increases in polar ice volume. By contrast, new discoveries from the middle and late Eocene of Peru reveal that penguins invaded low latitudes >30 million years earlier than prior data suggested, during one of the warmest intervals of the Cenozoic. A diverse fauna includes two new species, here reported from two of the best exemplars of Paleogene penguins yet recovered. The most comprehensive phylogenetic analysis of Sphenisciformes to date, combining morphological and molecular data, places the new species outside the extant penguin radiation (crown clade: Spheniscidae) and supports two separate dispersals to equatorial (paleolatitude $\approx 14^\circ\text{S}$) regions during greenhouse earth conditions. One new species, *Perudyptes devriesi*, is among the deepest divergences within Sphenisciformes. The second, *Icadyptes salasi*, is the most complete giant (>1.5 m standing height) penguin yet described. Both species provide critical information on early penguin cranial osteology, trends in penguin body size, and the evolution of the penguin flipper.

Aves | evolution | Peru | fossil | Bergmann's rule

Climate has been hypothesized to play a key role in evolutionary patterns of both living (1–5) and extinct penguins (4–9). Whereas the earliest penguins appear >60 Ma (10), extant lineages were recently proposed to originate in association with abrupt latest Eocene–Oligocene global cooling (≈ 34 Ma; see refs. 11 and 12) and to undergo a major radiation and range expansion to low latitudes only during later Neogene cooling (4). Extant penguin species are broadly considered to be cool-adapted, and even equatorial species are sensitive to sea surface temperature increases associated with El Niño Southern Oscillation events (13).

The new fossils are the first to indicate significant low-latitude penguin diversity over a period characterized by one of the most important climatic shifts in earth history: the transition from peak temperatures in the pre-Oligocene greenhouse earth to the development of icehouse earth conditions (11, 12). The fossils reveal key data on the poorly known pre-Miocene history of penguins in South America (6, 9, 14). The fauna, from new Eocene localities in Peru, includes the two new species as well as additional material indicating the

presence of at least five penguin taxa (ref. 15 and undescribed specimens). The only other pre-Oligocene penguin fossil from South America is a partial hindlimb from the high-latitude southernmost tip of the continent, equivalent in age to the middle Eocene Peruvian specimens (14). Together, these two records constitute the earliest for penguins on the continent.

Systematic Paleontology

Aves Linnaeus, 1758 (*sensu* Gauthier, 1986).

Neognathae Pycraft, 1900.

Sphenisciformes Sharpe, 1891 (*sensu* Clarke *et al.*, 2003).

***Perudyptes devriesi*.** New genus, new species.

Holotype specimen. Museum of San Marcos University, Peru (MUSM) 889, comprising a skull, mandible, cervical vertebrae and ribs, humeri, left carpometaacarpus, synsacrum, femora, right tibiotarsus, and left tarsometatarsus (Fig. 1).

Etymology. “Peru” references the fossil provenance, and “dyptes” is Greek for diver. The species name “devriesi” honors Tom DeVries, whose dedicated work and longstanding collaboration in the Pisco Basin of Peru made possible the discovery of the new localities and species.

Locality and age. MUSM 889 is from a coarse-grained, thick-bedded, siliciclastic sandstone exposed at Quebrada Perdida ($14^\circ 34'\text{S}$, $75^\circ 52'\text{W}$), Department of Ica, Peru, identified to the basal portion of the middle to late Eocene Paracas Formation (16). The presence of the gastropod *Turritella lagunillasensis* in correlative sandstone beds confirms the assignment of the holotype locality to the basal Paracas Formation (16, 17), as does the discovery of late middle Eocene radiolarians (*Cryptocarpium ornatum*, *Lithocyclus aristotelis*, and *Lithocyclus ocellus*) in tuffaceous fine-grained sandstones much higher in the section (≈ 42 Ma).^k

Author contributions: J.A.C. and D.T.K. designed research; J.A.C., D.T.K., M.S., M.U., N.G., S.B., Y.N., and C.A.B. performed research; J.A.C., D.T.K., M.S., N.G., S.B., Y.N., and C.A.B. analyzed data; and J.A.C., D.T.K., M.S., N.G., S.B., and C.A.B. wrote the paper.

The authors declare no conflict of interest.

This article is a PNAS Direct Submission. R.E.F. is a guest editor invited by the Editorial Board.

Abbreviation: MUSM, Museum of San Marcos University, Peru.

^dTo whom correspondence should be addressed. E-mail: julia.clarke@ncsu.edu.

^kDeVries, T. J., Narváez, Y., Sanfilippo, A., Malumian, N., Tapia, P., XIII Congreso Peruano de Geología, Oct. 17–20, 2006, Lima, Perú (ext. abstr.).

This article contains supporting information online at www.pnas.org/cgi/content/full/0611099104/DC1.

© 2007 by The National Academy of Sciences of the USA

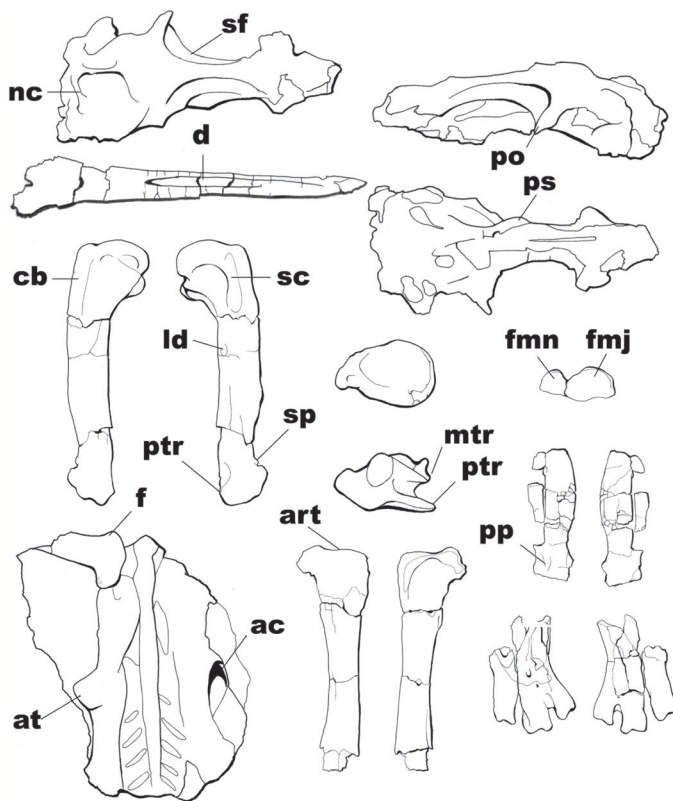


Fig. 1. Holotype of *P. devriesi* (MUSM 889). (a) Skull in dorsal view. (b) Skull in left lateral view. (c) Left dentary in medial view. (d) Skull in ventral view. (e) Right humerus in anterior and posterior views. (f) Right humerus in proximal view. (g) Right humerus in distal view. (h) Left carpometacarpus in distal view. (i) Left carpometacarpus in ventral and dorsal views. (j) Synsacrum, ilia, and left femur in dorsal view. (k) Right femur in posterior and anterior views. (l) Left tarsometatarsus in plantar and dorsal views. All to same scale except j (scale for j is at lower left); f, g, and h are enlarged in the line drawings to show detail. Anatomical abbreviations: ac, acetabulum; art, articular surface for antitrochanter; at, antitrochanter; cb, coracobrachialis insertion; d, depression on lingual surface of dentary; f, femur; fmn, articular facet for first digit of metacarpal III; fmj, articular facet for first digit of metacarpal II; ld, scar for latissimus dorsi; mtr, middle trochlear ridge; nc, nuchal crest; po, postorbital process; pp, pisiform process; ps, expansion of parasphenoid; ptr, posterior trochlear ridge; sc, scar for supracoracoideus; sf, fossa for salt gland; sp, supracondylar tubercle.

Diagnosis. *P. devriesi* is diagnosed by the following four autapomorphies relative to all other Sphenisciformes: (i) postorbital process directed anteroventrally; (ii) marked anterior expansion of the parasphenoid rostrum; (iii) posterior ridge forming the humeral scapulotriceps groove projects distal to the middle ridge and is conformed as a large, broadly curved surface; and (iv) femur with a convex articular surface for the antitrochanter. Additional differential diagnosis is given in [supporting information \(SI\) Appendix](#).

Description. Deep temporal fossae excavate the skull roof, and the frontal is beveled for a supraorbital salt gland. A pronounced sagittal crest meets the nuchal crest at a 90° angle. The postorbital process is directed anteroventrally, unlike the ventral orientation in other penguins. The nasal-premaxilla suture is obliterated. The left mandible indicates a straight, elongate beak with a short symphysis. A lingually directed flange from the dorsal margin expands to create a flat surface, a feature previously unknown in penguins. An elongate depression on the lingual surface of the dentary is similar to a feature present in Gaviidae (loons) and to an Eocene sphenisciform mandible (18); extant penguins lack this morphology.

The humerus is flattened and pachyostotic. The dorsal tubercle is nearly level with the apex of the head. The shaft is narrow and lacks notable distal expansion. The coracobrachialis impression is developed as a shallow oblong fossa, and the tricipital fossa is deep, undivided, and apneumatic. The supracoracoideus insertion scar is elongate and well separated from the small,

circular latissimus dorsi insertion scar. A compact dorsal supracondylar tubercle is present, a feature absent in all other penguins except the basal taxon *Waimanu* (10). The ulnar condyle is damaged, but a wide shelf-like surface is preserved adjacent to the posterior margin of the condyle. Metacarpal II is anteriorly bowed, with a broad anterior margin unlike the compressed sharp edge present in extant penguins. The pisiform process is a low but distinct ridge. The articular facet for the phalanx of metacarpal III is plesiomorphically subtriangular. The sutures between the ilia and the sacrum are open. The femur has a very weak trochanteric crest and is nearly straight for its preserved length. A proximally placed fibular crest and narrow supratendinal bridge are discernable on the tibiotarsus. The tarsometatarsus is short, with a straight metatarsal IV and a shallow dorsal sulcus between metatarsals II and III. The medial proximal vascular foramen and the distal vascular foramen are absent.

***Icadyptes salasi*.** New genus, new species.

Holotype specimen. MUSM 897, comprising a skull, axis, and eight additional cervical vertebrae, partial right and left coracoids, cranial end of the left scapula, left humerus, radius, ulna, proximal carpals, carpometacarpus, and phalanges (Fig. 2).

Etymology. “Ica” refers to the Department of Ica, “dyptes” is Greek for diver. “Salasi,” honors Rodolfo Salas for his important contributions to vertebrate paleontology in Peru.

Locality and age. MUSM 897 is from a tuffaceous, diatomaceous, fine-grained sandstone that is part of the basal transgressive

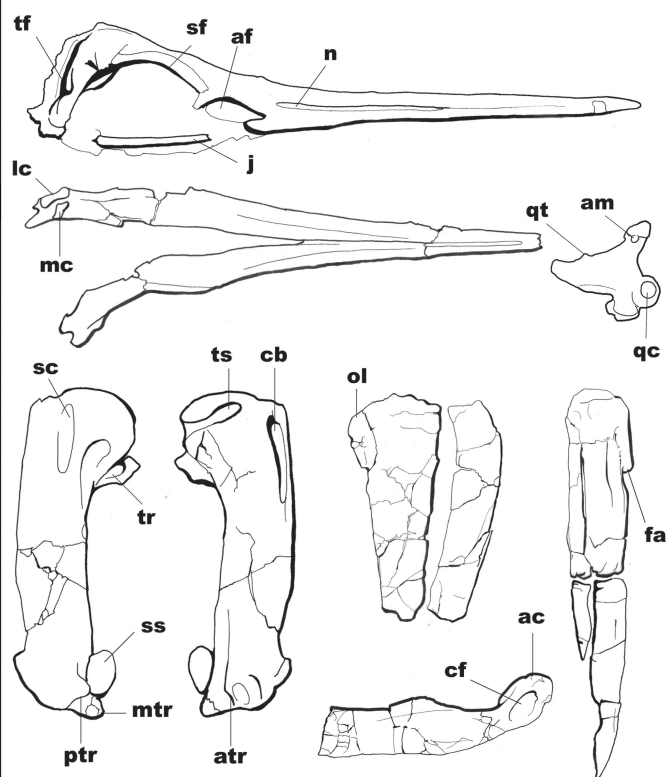


Fig. 2. Holotype of *I. salasi* (MUSM 897). (a) Skull in lateral view. (b) Mandible in dorsal view. (c) Left quadrate in lateral view. (d) Left humerus in posterior and anterior views. (e) Left ulna in ventral view. (f) Left radius in ventral view. (g) Left carpometacarpus and phalanges in ventral view. (h) Left coracoid in ventral view. All are to the same scale except c, which is enlarged to show detail. Anatomical abbreviations: ac, acrocoracoid process; af, anteorbital fenestra; am, tubercle for m. adductor mandibulae externus; atr, anterior trochlear ridge; cb, coracobrachialis insertion; cf, ovoid coracoid fossa; fa, distal facet of first metacarpal; j, jugal; lc, lateral cotyle of mandible; mc, medial cotyle of mandible; mtr, middle trochlear ridge; n, nares; ol, olecranon; ptr, posterior trochlear ridge; qc, quadratojugal cotyle; qt, tubercle on optic process; sc, scar for supracoracoideus; sf, fossa for salt gland; ss, sesamoid of m. scapulotriceps tendon; tf, temporal fossa; tr, tricipital fossa; ts, transverse sulcus.

sequence of the Otuma Formation (16)¹ exposed in the lower Ullujaya Valley of the Río Ica, Department of Ica (14°37'S, 75°37'W). The fossil-bearing unit lies 70 m above an angular unconformity marking the base of the depositional sequence. Specimens of the gastropods *Peruchilus culberti* and *Xenophora carditigera* establish a late-middle to late Eocene age for this sequence, whereas microfossils from a contiguous and continuous section indicate a more exact age of ≈ 36 Ma for the strata containing MUSM 897.¹ Additionally, ash beds collected near the base of the same depositional sequence 5 km southwest across the Río Ica yielded ⁴⁰Ar/³⁹Ar dates of 37.2 and 36.5 Ma, whereas an ash bed higher in the section, correlated with beds above the horizon bearing MUSM 897, yielded an age of 35.7 Ma.^k

Diagnosis. *I. salasi* possesses four proposed autapomorphies relative to all other penguins: (i) a beak forming more than two-thirds of the skull length, (ii) fusion of the premaxillae and palatines, (iii) axis with an elongate hypophysis terminating in a greatly mediolaterally expanded disk-like plate, and (iv) a deep ovoid fossa on the lateral surface of the acrocoracoid process. *I. salasi* is also differentiated from all other penguins by the following combination of postcranial characters: humerus with a straight, broad shaft (midshaft width/length = 0.22); metacarpal I with a flat carpal trochlea and distinct distal terminus; and

metacarpals II and III subequal in distal extent. Additional differential diagnosis is given in [SI Appendix](#).

Description. The skull of *I. salasi* is the first complete specimen reported for a basal penguin. Striking is the hyperelongate, spear-like beak, unlike that of any previously known extinct or extant penguins. Fusion of the palatal elements and premaxillae creates a powerfully constructed upper jaw with a flat ventral surface bounded by lateral ridges and inscribed with reticulate vascular sucli. Similar vascular texturing is seen in Sulidae (boobies and gannets) but is not present in other penguins, suggesting a distinct rhamphotheca in *I. salasi*. The mandible has an extensive symphysis with a corresponding flat dorsal surface. The cranium is extremely narrow, with deep temporal fossae meeting at a midline sagittal crest. A supraorbital shelf for the salt gland is present. The external nares extend posterior to the anterior margin of the antorbital fenestra. The jugal bar is straight. The pterygoid is rod-like, lacking the fan-like anterior expansion present in Spheniscidae. The otic process of the quadrate is shorter than the optic process. The quadrate shaft bears a tubercle for the adductor mandibulae externus attachment that abuts the squamosal capitulum. A retroarticular process is present.

The axis is mediolaterally compressed and elongate compared with extant penguins, and the remaining cervical vertebrae are robust, particularly compared with the narrow skull. The coracoids preserve deep scapular cotylae, and the scapula shares the expanded proximal end present in extant penguins. The humeral supracoracoideus scar parallels the long axis of its shaft, and the

¹DeVries, T. J., XII Congreso Peruano de Geología, Oct. 26–29, 2004, Lima, Perú (ext. abstr.).

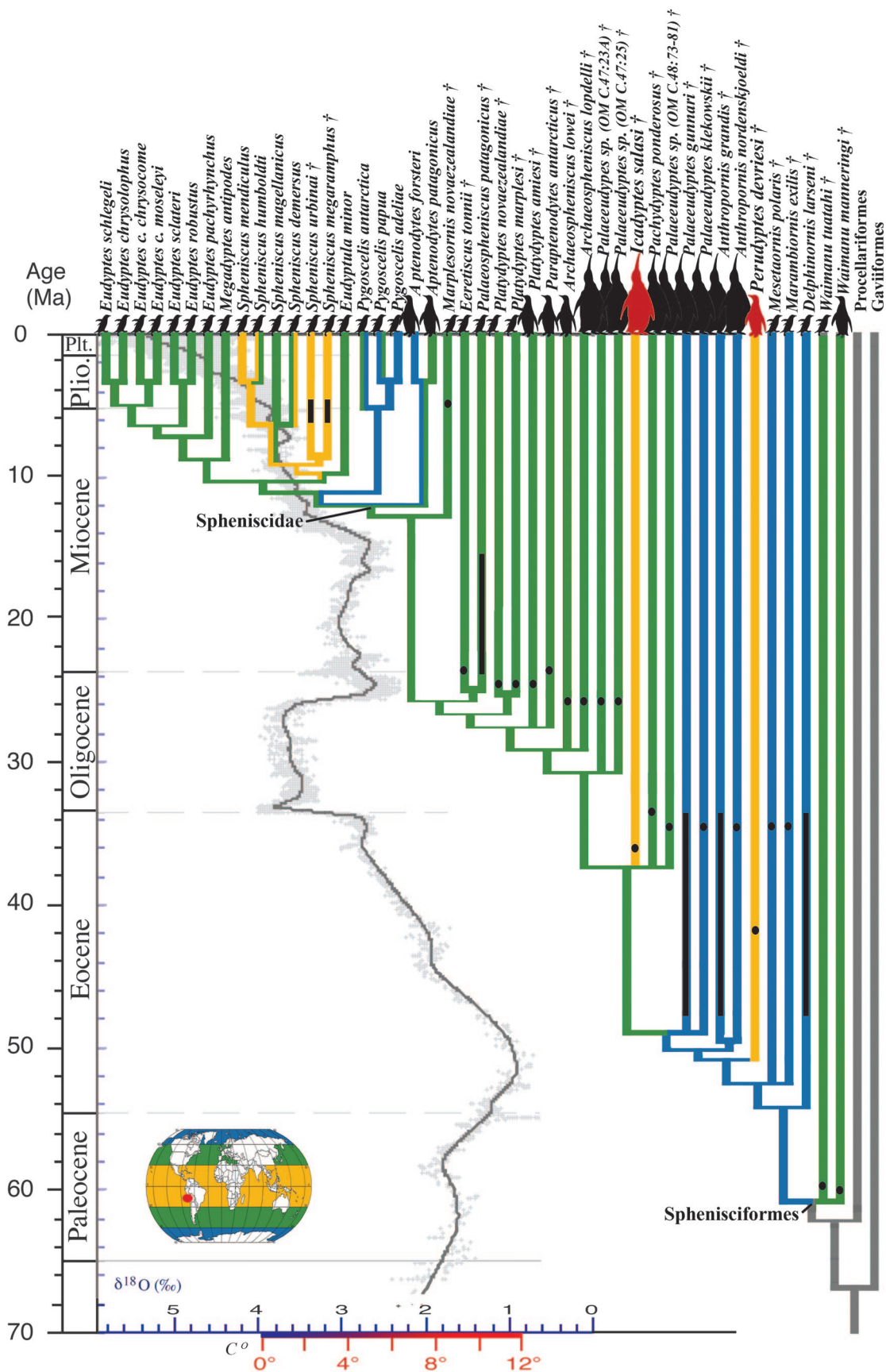


Fig. 3. Recovered penguin phylogenetic relationships, including placement of new species *P. devriesi* and *I. salasi* (in red) and showing stratigraphic and latitudinal distribution of species against $\delta^{18}\text{O}$ values as a proxy for changes in global temperature over the last 65 Ma (from ref. 12). The strict consensus cladogram of the four most parsimonious trees (4,356 steps) is shown. Black bars indicate stratigraphic range. No neospecies has a fossil record extending beyond

latissimus dorsi insertion is displaced distally to near midshaft. The tricipital fossa is undivided. Two distal trochlea are present for the humerotriceps and scapulotriceps sesamoids. The ulnar olecranon process is tab-like and proximally located, as in *Waimanu* (10) and *Palaeudyptes* (19). The radius bears a roughened anteroproximal brachialis insertion surface but lacks a proximally directed process on the anterior border. Metacarpals II and III are equal in distal extent as in some other Paleogene species, whereas in extant and most extinct species metacarpal III extends farther. A free alular digit is absent. Phalanx II-1 is longer than phalanx III-1, unlike in extant penguins in which these two digits are subequal in length.

Penguin Evolution and Cenozoic Climate Change

Phylogenetic results from analysis of the largest data set yet compiled for penguins, following the combined analysis methods of ref. 20, identify *P. devriesi* as a deep divergence within penguins and *I. salasi* as part of a paraphyletic assemblage of giant Eocene–Oligocene taxa closer to Spheniscidae, the penguin crown clade (Fig. 3). Relationships among extant genera are those recovered from less inclusive molecular data sets in maximum-likelihood and Bayesian analyses (4).

The Peruvian species inform estimates of Pacific biotic connections during greenhouse-to-icehouse earth transition. Two equatorial ingressions by Paleogene penguins are supported (Fig. 3). On the basis of ancestral area reconstructions (see *SI Appendix*), one dispersal from Antarctic regions is inferred by the middle Eocene and a second from New Zealand by the late Eocene. Whether this biogeographical pattern reflects proposed, but controversial, late Eocene (≈ 41 Ma; ref. 21) beginnings for reorganization of southern ocean circulation patterns and isolation of Antarctica (21) deserves further investigation.

We find no fossil evidence for the extant penguin radiation, Spheniscidae, earlier than a species of *Spheniscus* ≈ 8 million years in age (22); all pre-late Miocene taxa are placed outside this radiation (Fig. 3). By contrast, molecular sequence divergence estimates identify the origin of this radiation at 40 Ma (4). Although there is an extensive sphenisciform fossil record from multiple continents between 40 and 8 Ma, no fossil from this interval has been placed as part of Spheniscidae (refs. 6 and 23 and Fig. 3). Calculations from modified scripts for MSM*range (ref. 24 and see *Materials and Methods*) indicate that accommodation of the molecular divergence estimates would require an additional 164.1–334.2 million years of missing fossil record (a 172–205% increase) compared with the inferred missing record (“ghost lineages”) given only cladogram topology and fossil ages. The fossil record of penguins is approximately three times as incomplete when divergence dates are required to be true and would be strikingly biased toward recovery of only stem taxa.

Extant penguin diversification may be related to later Neogene global cooling phases (4, 12), but there is no fossil evidence to support a crown radiation in the Paleogene concomitant with the initiation of the circum-Antarctic current, initial onset of Cenozoic global cooling, or at the proposed extinction of giant penguins (in contrast to ref. 4). An Oligocene fossil cited as representing the extant genus *Eudyptula* in support of a Paleogene crown radiation (4) is not assignable to that genus (6). Although stratigraphic data can only falsify a divergence date when a fossil discovery is older than estimated, the large amount of implied missing fossil record suggests that proposed crown

penguin divergence times may be too old. Future analyses using calibration points within the crown clade (e.g., refs. 22 and 25) could improve the fit of these estimates.

Based on inferred patterns linking latitudinal expansion, increases in extant species diversity, and phases of Cenozoic global cooling, it was predicted (4) that global warming could trigger an opposite pattern in the penguin lineage, with equatorial species retreating to higher latitudes and high-latitude species facing extinction. This prediction is supported by data on some extant species (1, 3). The new Peruvian species indicate that early in penguin evolution there was a more complex relationship between global temperature and diversity than previously recognized. Additional factors such as upwelling (26) and ocean circulation patterns (6, 20, 23) were also critical in the evolution of the penguin lineage. Because the Peruvian species are members of the stem sphenisciform lineage and current global warming would be on a distinct, significantly shorter time scale, the data from these basal forms should not be used to refute predictions of changes in extant penguin distribution with continued warming. Given the different interactions between climate and distribution seen in basal penguins and in extant species, the physiological and ecological factors that could drive the response of extant penguins to climate change (1, 3, 13) may well be restricted to the crown clade.

Body Size Evolution

The phylogenetic results are consistent with a single origin of extremely large size in the penguin lineage (in contrast to ref. 27) by the early Eocene and retained in *Icadyptes*. Giant size persisted into the Oligocene (6, 19) across the Eocene–Oligocene climate transition (Fig. 3). Intriguingly, over late Tertiary global cooling, the average size of penguins has become smaller (Fig. 3).

Icadyptes was far larger than any living penguin, whereas *Perudyptes* was approximately the size of the extant king penguin. Compared with the three largest previously described extinct taxa, the *I. salasi* holotype humerus is ≈ 5 mm shorter than the largest exemplars of *Pachydyptes ponderosus* (19) and *Anthropornis nordenskjoeldi* (8, 28) and exceeds the largest of *Palaeudyptes klekowskii* (28) by ≈ 9 mm. Regressions based on hindlimb measurements estimated the standing height and mass of *A. nordenskjoeldi* (1.66–1.99 m and 81.7–97.8 kg, respectively) and of *P. klekowskii* (1.47–1.75 m and 56.0–65.7 kg, respectively) (29). Humeral dimensions indicate that the holotype individual of *I. salasi* would be intermediate in size between these two taxa, yielding a conservative minimum standing height of 1.5 m.

When the body size of low-latitude *I. salasi* is compared with all higher latitude taxa with overlapping observed and inferred stratigraphic ranges (Fig. 3), *I. salasi* is larger or approximately the same size. Although body size distribution in birds has been suggested to be largely consistent with the proposed biological law “Bergmann’s rule,” relating cooler temperatures and higher latitudes with large body size (e.g., refs. 30 and 31; although, see ref. 32), the warm water foraminiferan *Asterigerina* has been recovered in matrix associated with giant-form *P. ponderosus*, a form approximately the same size as *Icadyptes* (19). Giant size in the penguin lineage does not appear to be correlated with either cooler temperatures or higher latitudes. A period of increased late Eocene upwelling (11) and ocean productivity that would have impacted the Peruvian coast (26) should be investigated as

the Pleistocene (6). Extinct taxa are indicated with a †. Branch color indicates the latitude of extant taxon breeding territories and the paleolatitude of fossil taxon localities, with ancestral latitude ranges reconstructed along internal branches from downpass optimization: 0–30°S latitude (yellow), 30–60° (green), and 60–90° (blue). Silhouettes reflect body size; small silhouettes indicate taxa smaller than extant *Aptenodytes patagonicus* (king penguin), medium silhouettes indicate taxa intermediate between *A. patagonicus* and *Aptenodytes forsteri* (emperor penguin), and large silhouettes indicate taxa larger than *A. forsteri*. The plot of mean $\delta^{18}\text{O}$ values and estimated mean ocean water temperature scale (only valid for an ice-free ocean, preceding major Antarctic glaciation at ≈ 35 Ma) are from ref. 12 and give an indication of changing conditions across the Cenozoic.

a potentially important factor driving low-latitude penguin species diversity and body size.

Implications for the Evolution of Penguin Morphology

The Peruvian fossils provide insight into early penguin cranial anatomy and the evolution of the penguin flipper apparatus. An elongate, powerfully constructed beak unknown in extant penguins is present in both *Perudyptes* and *Waimanu* (10) and, in an extreme form, in *Icadyptes*. This morphology can now optimized as ancestral for penguins. Undescribed long-billed Oligocene fossils have also been reported (6, 10), revealing that this morphology was retained for a significant portion of early penguin evolution and through the greenhouse-to-icehouse transition (12).

Perudyptes displays a unique combination of traits that fills an important gap between the wing morphology of the basal-most penguin, *Waimanu*, and living penguins. The extant penguin wing is highly modified into a stiffened, paddle-like structure equipped with a greatly reduced set of intrinsic wing muscles (33) and exhibiting the lowest degree of intrinsic joint mobility of any extant avian group (34). The presence of a conspicuous dorsal supracondylar tubercle and distinct pisiform process in *Perudyptes* are consistent with retention of functioning major intrinsic wing muscles whose attachment surface (extensor carpi radialis) and pulley-like guide (flexor digitorum profundus) these processes represent. In penguins closer to and including the crown clade, the dorsal supracondylar tubercle is absent, with indication of muscle origin reduced to a weak, flat scar. The pisiform process is reduced to a barely perceptible ridge. Like other basal penguins, *Perudyptes* retains a prominent ulnar condyle that potentially permitted greater flexion at the humerus-ulna joint, although the large shelf adjacent to the condyle would restrict flexion during the flight downstroke (23). New data from the Peruvian fossils invite further biomechanical research to discern implications for locomotor differences and feeding ecology in basal penguins.

Conclusions

With the discovery of the new Peruvian species, penguins show a much more complex relationship with climate factors early in their evolution. Inference of ancestral vs. extant ecologies within a lineage, and attention to when in that lineage derived characteristics arose, are key to qualifying interpretations relating past biotic events causally to climate shifts, as well as to informing predictions for future responses to change. Although molecular

divergence dating approaches offer great insight into the timing and potential causal factors in lineage diversification, case studies evaluating groups with a comparably rich record offer the only available test to these scenarios. In the case of the penguin lineage, a much more complex paleobiogeographical pattern and grossly different timing of key origin and radiation events are indicated, at odds with current divergence dating estimates.

Materials and Methods

Phylogenetic Analysis and Ancestral Area/Latitude Reconstruction.

The data set comprised 194 morphological characters sampled for 43 fossil and living penguin taxa and ≈ 6.5 kbp from five genes (*RAG-1*, *12S*, *16S*, *COI*, and *cyt-b*) for all extant penguins. Direct optimization methods and search strategy follow ref. 20, with 200 tree bisection and reconnection replicates conducted in POY (version 3.0.11; American Museum of Natural History). See [SI Data Set](#) and [SI Appendix](#) for matrix, GenBank accession numbers, Bremer support values, area and latitude categories, and references for fossil ages.

Missing Fossil Range Calculation. MSM*range (24), a method used to compare the temporal order of successive branching events with the age of appearance of terminal taxa in the stratigraphic record, was adapted to analyze the effects of requiring the divergence times estimated from calibrated molecular sequence data (4). Ancestral nodes, and associated inferred divergence dates, were incorporated into the analyzed Newick tree. The range of missing record reflects the iterative first appearance datum sampling procedure used by MSM*range and different resolutions of polytomies in our consensus tree.

We thank T. DeVries for stratigraphic data and for many contributions to Peruvian geology and paleontology; R. Salas, N. Valencia, D. Omura, W. Aguirre, and E. Díaz, for fieldwork assistance and fossil preparation; L. Brand and C. Aguirre for contributions to fieldwork; K. Lamm for illustrations; T. Ando and R.E.F. for information on *Waimanu*; P. Goloboff for supercluster access; and the editor and two anonymous reviewers for comments that improved our manuscript. We are grateful for support provided by the National Science Foundation Office of International Science and Engineering, National Geographic Society Expeditions Council, North Carolina State University, and North Carolina Museum of Natural Sciences (J.A.C.); The Frank M. Chapman Memorial Fund, The Doris O. and Samuel P. Welles Research Fund, and American Museum of Natural History Division of Paleontology (D.T.K.); and the National Science Foundation Assembling the Tree of Life Project: Archosaur Phylogeny.

1. Forcada J, Trathan PN, Reid K, Croxall JP (2006) *Glob Change Biol* 12:411–423.

2. Croxall JP, Trathan PN, Murphy EJ (2002) *Science* 297:1510–1514.

3. Barbraud C, Weimerskirch H (2001) *Nature* 411:183–186.

4. Baker AJ, Pereira SL, Haddrath OP, Edge KA (2006) *Proc R Soc London Ser B* 212:11–17.

5. Williams TD (1995) *The Penguins* (Oxford Univ Press, Oxford).

6. Fordyce RE, Jones CM (1990) in *Penguin Biology*, eds Davis LS, Darby JT (Academic, San Diego), pp 419–446.

7. Jenkins RJF (1974) *Paleontology* 17:291–310.

8. Simpson GG (1971) *Bull Am Mus Nat Hist* 144:319–378.

9. Simpson GG (1946) *Bull Am Mus Nat Hist* 87:7–99.

10. Slack KE, Jones CM, Ando T, Harrison GL, Fordyce RE, Arnason U, Penny D (2006) *Mol Biol Evol* 23:1144–1155.

11. Tripathi A, Backman J, Elderfield H, Ferretti P (2005) *Nature* 436:341–346.

12. Zachos J, Pagani M, Sloan L, Thomas E, Billups K (2001) *Science* 292:686–693.

13. Boersma PD (1998) *Condor* 100:245–253.

14. Clarke JA, Olivero EB, Puerta P (2003) *Am Mus Novit* 3423:1–18.

15. Acosta Hospitaleche C, Stucchi M (2005) *Revista de la Sociedad Española de Paleontología* 20:1–6.

16. DeVries TJ (1998) *S Am Earth Sci* 1:217–231.

17. Rivera R (1957) *Bol Soc Geol Perú* 32:165–220.

18. Olson SL (1985) *Avian Biol* 8:79–238.

19. Marples BJ (1952) *N Z Geol Surv Paleontol Bull* 20:1–66.

20. Bertelli S, Giannini NP (2005) *Cladistics* 21:209–239.

21. Scher HD, Martin E (2006) *Science* 312:428–430.

22. Stucchi M (2002) *Bol Soc Geol Perú* 94:17–24.

23. Ksepka DT, Bertelli S, Giannini NP (2006) *Cladistics* 22:412–441.

24. Pol D, Norell M (2006) *Syst Biol* 55:512–521.

25. Walsh SA, Suárez ME (2006) *Hist Biol* 18:115–126.

26. Hartley AJ, Chong G, Houston J, Mather AE (2005) *J Geol Soc (London)* 162:421–424.

27. Tambussi CP, Reguero MA, Marensi SA, Santillana SN (2005) *Geobios* 38:667–675.

28. Jadwiszczak P (2006) *Polish Polar Res* 27:3–62.

29. Jadwiszczak P (2001) *Polish Polar Res* 22:147–158.

30. Ashton KG (2002) *Global Ecol Biogeogr* 11:505–523.

31. Meiri S, Dayan T (2003) *J Biogeogr* 30:331–351.

32. Zink RM, Remson JV, Jr (1986) in *Current Ornithology*, ed Johnston RF (Plenum, New York), Vol 4, pp 1–69.

33. Raikow RJ, Bicanovsky L, Bledsoe AH (1988) *Auk* 105:446–451.

34. Schreiweis DO (1982) *Smithsonian Contrib Zool* 341:1–46.